

# Spin-specific photoelectron diffraction, photoelectron spectroscopy, and absorption using magnetic x-ray circular dichroism

J. G. Tobin

*Chemistry and Materials Science Department, Lawrence Livermore National Laboratory, Livermore, California 94550*

G. D. Waddill

*Department of Physics, University of Missouri–Rolla, Rolla, Missouri 65401-0249*

D. P. Pappas

*Department of Physics, Virginia Commonwealth University, Richmond, Virginia 23284-2000*

E. Tamura

*Chemistry and Materials Science Department, Lawrence Livermore National Laboratory, Livermore, California 94550*

P. A. Sterne

*University of California, Davis, California 95616*

X. Guo and S. Y. Tong

*Laboratory for Surface Studies and Department of Physics, University of Wisconsin–Milwaukee, Milwaukee, Wisconsin 53201*

(Received 23 August 1994; accepted 27 February 1995)

We have helped to develop novel synchrotron-radiation-based techniques, using circularly polarized x rays. Photoelectron spectroscopy, photoelectron diffraction, and x-ray absorption variants will be discussed. From these, we are working to establish the structure–property relationships in nanoscale magnetic systems. © 1995 American Vacuum Society.

## I. INTRODUCTION

The magnetic properties of nanoscale (10–9 m) systems are of significance both because of their intrinsic scientific importance and the potential commercial exploitation of advances in magnetic technology. As the sophistication of synthesis and processing has increased and the device size has decreased, new tools have been required to characterize properties and structures on the nanoscale. A powerful new class of techniques has been developed, based upon the application of the tunable and circularly polarized x rays available from synchrotron-radiation sources. It is now possible to utilize the combined elemental selectivity and spin sensitivity of these core-level spectroscopies to obtain element-specific magnetic moments, exchange and spin-orbit splittings, and atomic-scale magnetic structures.

As an example of economic significance, consider the case of magnetic recording device read head technology.<sup>1,2</sup> Presently, magnetoresistive (MR) heads are replacing inductive heads, with a significant improvement in sensitivity. But today's MR heads are based upon Permalloy, with only a 2.5% MR effect. This pales in comparison with the much larger effects previously observed in spin-valve (10%)<sup>3</sup> and giant-magnetoresistive [(GMR), 150%]<sup>4–6</sup> systems. In fact, IBM is already developing GMR prototype devices.<sup>7–9</sup> Larger effects generally mean greater sensitivity, which will ultimately translate into smaller devices, one of the key ingredients in successfully competing in the multibillion-dollar-per-year magnetic-recording market.

The new spin-valve<sup>3</sup> and GMR systems<sup>4–6</sup> are composite materials, made up of various layers or imbedded granular deposits. The different layers or agglomerations are, in turn,

composed of different alloys and mixtures of elements. The interfacial regions between the layers or the granules and host materials are of great importance. It may be that most of the physics that gives rise to the unique properties of these materials occurs at the interfaces and is intimately coupled to the nanoscale dimensioning of the layers and granules, possibly connected to a Ruderman–Kittel–Kasuya–Yosida (RKKY) picture.<sup>9</sup> Nevertheless, the details remain unclear: for example, two schools of thought have already developed, one favoring the use of perfectly abrupt interfaces<sup>10</sup> and the other arguing for intermixed structures.<sup>11</sup> To resolve this dispute and ultimately determine the details that govern these effects, it is desirable to apply techniques which intimately combine elemental selectivity, spin specificity and a sensitivity to atomic-scale magnetic structure. As will be shown next, these requirements can be met by using techniques based upon core-level spectroscopies coupled with excitation by circularly polarized, tunable x rays.

The new family of techniques is based upon magnetic x-ray circular dichroism (MXCD). Here, we will briefly discuss three classes of experiments: MXCD absorption, MXCD photoelectron spectroscopy, and MXCD photoelectron diffraction. From these it is possible to extract element-specific magnetic moments, decouple spin orbit and exchange splittings, respectively, and determine atomic-scale magnetic structure.

## II. EXPERIMENT

The experiments were performed at the Stanford Synchrotron Radiation Laboratory (SSRL) using a spherical grating monochromator capable of delivering from ~80% to ~90%

circularly polarized radiation. The beamline (BL 8–2) is based upon a spherical grating monochromator, which can operate in either high-resolution or circular polarization modes. It is also part of the UC/National Laboratory Facilities at SSRL.<sup>12</sup> Monolayer (ML) Fe films were grown on a Cu(001) substrate held at  $\sim 150$  K. This results in relatively poorly ordered metastable fcc Fe overlayers as evidenced by the diffuse  $p(1 \times 1)$  low-energy electron diffraction (LEED) pattern observed for these films. At low coverages, these films have a magnetic easy axis along the sample normal and were magnetized *in situ* with an electromagnet coil. All measurements were made in remanence. The spectra were collected with an angle-resolving hemispherical analyzer<sup>12</sup> with angular acceptance of  $\pm 3^\circ$ . The magnetic axis dictated that the spin-dependent effects were optimized for photons incident along the sample normal. The analyzer position was adjusted to the desired electron emission angle. Generally, the collection plane coincided with the orbital plane of the storage ring, i.e., the horizontal plane. Angular alignment was determined using LEED and laser reflection.

### III. MXCD ABSORPTION

Let us now consider the absorption of an x ray with the concurrent excitation of an electron from a core level. Because core-level binding energies are element specific, a tunable x-ray source automatically permits a controlled, selective examination on an element-by-element basis. Moreover, the localization of tightly bound core levels encourages the dominance of electric-dipole selection rules.<sup>13,14</sup> It is the combination of strong dipole selection rules and variable circular polarization that allows a direct specificity of the spin of the excited electrons, without having to resort to the low efficiency spin-polarizing detectors.<sup>15</sup>

A manifestation of these strong selection rules can be seen in Fig. 1. Here, the process is x-ray absorption in 2 monolayers of Fe on Cu(001). The strong dichroism, i.e., spectral changes between the parallel and antiparallel configurations, is a result of combination of the dipole selection rules and the high degree of spin polarization in the unoccupied conduction bands. In x-ray absorption, the number of photons absorbed is measured as a function of photon energy, particularly as the threshold energy (binding energy) of a specific core level is attained. At threshold, the excitation is into the lowest energy unoccupied states. In magnetic materials, these states are highly spin polarized and dense. Thus in Fe, the  $2p$  to  $3d$  transitions show “white lines” or peaks, not just steps, at the thresholds. Because the empty conduction states are spin polarized and of specific orbital quantum number distribution, the white line peak intensity varies with both circular polarization and the angular momentum quantum numbers of the excited electron. Hence we see reversed effects at the  $L_{III}(2p_{3/2})$  and  $L_{II}(2p_{1/2})$  edges. Strong dichroisms such as this have been observed in a number of overlayer,<sup>14</sup> multilayer,<sup>16</sup> and bulk<sup>17</sup> systems. It has also been shown that, for at least some cases, both the spin<sup>14,18</sup> and orbital<sup>16,19</sup> moment can be directly determined from such spectra using “sum rules.” This is intuitively appealing because the polarization of the conduction bands is inherently coupled to the magnetic moment, but further work will be

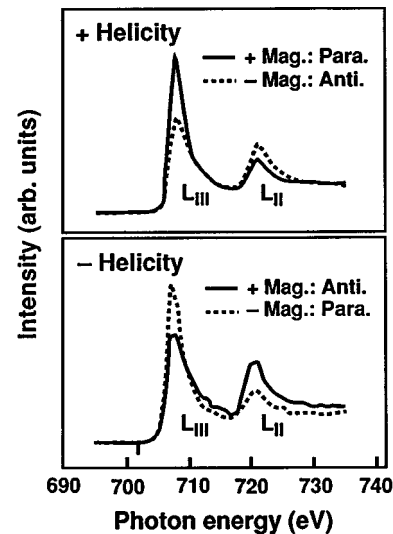


FIG. 1. MXCD-x-ray absorption for the Fe  $2p \rightarrow 3d$  transitions. The near-edge x-ray-absorption fine-structure (NEXAFS) dichroism of 2 ML of Fe/Cu(001). These are plots of absorption versus photon energy. The upper panel shows the effect of reversing the magnetization while maintaining the positive helicity of x rays. Similarly, for the lower panel and negative helicity x rays. Samples are perpendicularly magnetized either into (positive magnetization) or out of (negative magnetization) the surface. The symbol para(anti) means that the helicity and magnetization are parallel (antiparallel). The  $2p_{3/2}$  peak is at the  $L_{III}$  edge and the  $2p_{1/2}$  peak is at the  $L_{II}$  edge. The strong were normalized to each other by equating the pre-edge intensity, at energies below approximately 700 eV. In x-ray absorption, there is the observation of strong dichroic effects. (From Ref. 14.)

necessary to properly quantify the impact of complicating factors such as delocalization and multielectronic effects.<sup>20</sup>

A particularly simple relation, applicable to localized  $3d$  magnetic systems with strong orbital quenching and a large spin moment, is shown in Table I. Here BR is the branching ratio, i.e., the intensity of the  $2p_{3/2}$  peak divided by the sum of the  $2p_{3/2}$  and  $2p_{1/2}$  peak intensities. In fact, this expression can be viewed as a limiting case of the sum rule expressions.

### IV. MXCD PHOTOELECTRON SPECTROSCOPY

Just as the electric dipole selection rules give rise to strong dichroisms in the near-edge x-ray absorption spectra, they also produce strong polarized beams of photoelectrons. In photoelectron spectroscopy, the energies have been increased to cause actual ejection of the core-level electrons. Because of the dipole selection rules, there will be strongly polarized emission. In the case of the Fe  $2p$ , we would naively expect  $\pm 25\%$  for the  $2p_{3/2}$  and  $\mp 50\%$  for the  $2p_{1/2}$  level. These numbers are for parallel and antiparallel alignment of the photon helicity and magnetization, and represent an average over each manifold. Within each manifold, i.e.,  $2p_{3/2}$  or  $2p_{1/2}$  peak, individual multiplet structures can have much larger polarizations. The magnetic quantum number

TABLE I. Branching ratio (BR) analysis. ( $\mu$ =magnetic moment;  $n$ =number of valence  $d$  electrons;  $p_{hv}$ =photon polarization, circular).

$$\mu_{\text{spin}}^{\text{BR}} = \frac{4(10-n)}{P_{hv}} \left( \frac{\text{BR}^p - \text{BR}^a}{\text{BR}^p + \text{BR}^a} \right)$$

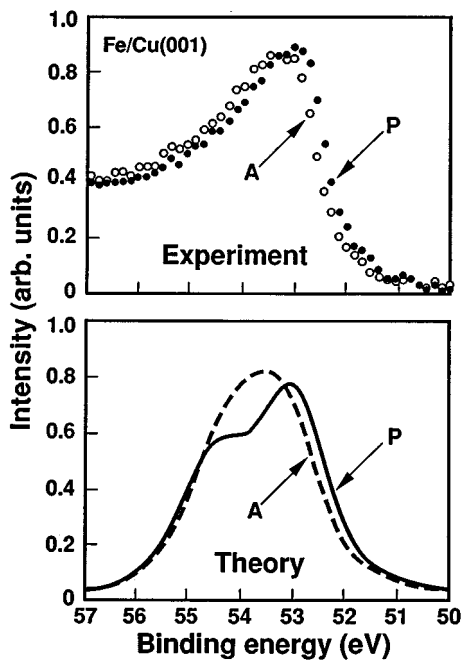


Fig. 2. Fe  $3p$  photoemission at  $h\nu=160$  eV, inside circularly polarized x rays. The experimental and theoretical photoemission spectra emitted from the  $3p$  state of the Fe/Cu(001) surface by left-handed circularly polarized (positive helicity) light of 160 eV incident normally. The magnetic moment vector is parallel (the solid circle and the solid line) or antiparallel (the open circles and the dashed line) to the light helicity. Here the information is principally in the front edge of the peaks, independent of the tailing asymmetry of the Doniach–Sunjic line shape. The theoretical results can be summarized as follows: spin-orbit splitting = 1.0–1.2 eV and exchange splitting = 0.9–1.0 eV. (From Ref. 24.)

states that give rise to the multiplet structure are shifted not only because of the spin-orbit interaction but also because of the exchange splitting. In the  $2p$  doublet, the exchange splitting manifests itself as a small shift ( $\sim 0.2$ – $0.5$  eV) on top of the much larger spin-orbit splitting ( $\sim 13$  eV).<sup>21,22</sup> But it would be wrong to assign the exchange splitting a value of 0.2 eV based upon such a crude analysis.

To extract spin-orbit and exchange splittings accurately and thus provide a meaningful benchmark for modelling of magnetic systems, it is necessary to simulate the spectra properly, including emission direction effects.<sup>23</sup> Shown in Fig. 2 is a difficult case, the Fe  $3p$ , where the spin-orbit and exchange splittings are both on the order of an eV. Using fully relativistic, spin-specific and multiple-scattering calculations, it is possible to mimic experimental results.

However, before comparing the experimental and theoretical results, it is appropriate to briefly consider our theoretical approach (for a more detailed description, including references, see Ref. 24). Neglecting scattering between photoelectrons and their holes in the photoexcitation process, the spin density matrix of the photoelectrons can be written in the form

$$\rho_{\sigma\sigma'} = -\frac{1}{\pi} v_e \langle \psi^\sigma | \Delta \text{Im} G \Delta^\dagger | \psi^{\sigma'} \rangle, \quad (1)$$

where  $|\psi^\sigma\rangle$  is the time-reversed LEED state for spin  $\sigma$ ,  $G$  the single-hole Green function, and  $v_e$  the velocity of the pho-

toelectrons. The electron–photon interaction  $\Delta$  is well approximated here by the dipole form and the intensity and spin polarization of photoelectrons are obtained from the spin density matrix. Although the photocurrent can be fully described by the single-hole Green function, it is difficult to renormalize the Green function to account for the many-body interaction between the hole and the other crystal electrons. For delocalized systems like metallic Fe, the problem is complicated and has been studied only for the free-electron system, in which the line spectra are modified with a Doniach–Sunjic (DS) line shape characterized by a singularity parameter. Since a DS line-shape modification does not affect the positions of lines in the multiplet structures, we have not included this type of many-body effect in our calculations. Many-body effects are included in our calculation in two different ways. First, finite hole lifetime effects are included through an imaginary part of the optical potential in the hole Green function, broadening the discrete energy eigenstates into a continuous spectrum. Second, the effective potentials (i.e., self-energy correction) for the  $3p$  holes are expected to be strongly energy (state) dependent and act differently on the majority and minority spins so that the effective spin-orbit and exchange splittings can be modified from the ground-state values in the photoexcitation process. Instead of estimating the effective potentials in a many-electron theory, we treat these splittings and a center binding energy of the  $3p$  holes as adjustable parameters and determine them by comparing to the experimental spectra. The magnetic Dirac equation based on density functional theory is accordingly modified in the core-state calculations. The exchange splitting is reduced by renormalizing the difference between the majority- and minority-spin ground-state potentials. For the spin-orbit interaction, we construct a quasirelativistic Dirac equation in which the strength of the spin-orbit coupling can be continuously tuned from the fully relativistic to the scalar relativistic Dirac equation. These approximations to the many-body effects allow us to take full advantage of the realistic final state wave function calculated by our fully relativistic multiple scattering computer code based on the layer Korringa–Kohn–Rostoker Green function method. An accurate representation of the final LEED state is very important, since it is known to be very energy sensitive in the low-energy region, and its character can change across the entire Fe  $3p$  linewidth, thereby altering the photoemission spectra.

Now, let us return to Fig. 2 and compare the experimental and theoretical spectra. Here, the information is in the leading edge of each peak: the asymmetrical experimental line shape is due to multielectron effects that cause the Doniach–Sunjic tails which, along the rising low kinetic energy (KE) tail and instrumental broadening, contribute to the obfuscation of the structure at higher binding energy. Nevertheless, from the comparison with previous linear dichroism<sup>15</sup> results and consistent with our observed peak shift of  $\sim 0.3$  eV, we can extract spin-orbit (1.0–1.2 eV) and exchange (0.9–1.0 eV) splittings.<sup>24</sup>

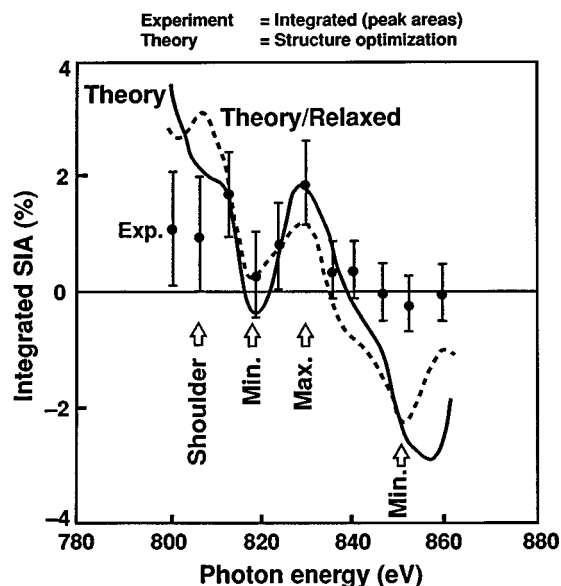


FIG. 3. Here is shown a comparison of experimental and theoretical results for spin-dependent photoelectron diffraction using magnetic x-ray circular dichroism. Calculated (solid curve:  $d_{12}=d_{23}=1.8 \text{ \AA}$ ,  $rp=0.19$ ; dashed curve:  $d_{12}=1.9 \text{ \AA}$ ,  $d_{23}=1.7 \text{ \AA}$ ,  $rp=0.17$ ) and measured intensity asymmetries along the [111] direction are shown as a function of photon energy. Representative error bars are included with the experimental data, shown as discrete values (triangles). The oscillatory behavior in the curves is due to spin-dependent photoelectron diffraction. It is the positions of the minima and maxima that is the crucial variation in photoelectron diffraction. Exact quantitative agreement will require higher signal to noise and refinement of the model structure. This is first structure determination with energy-dependent MXCD PD, performed by comparing integrated peak areas and a model including surface relaxation (dashed curve). (From Ref. 26.)

## V. MXCD PHOTOELECTRON DIFFRACTION

Perhaps the most important utilization of the spin-polarization photoelectrons will be for direct magnetic structure determination via photoelectron diffraction. It has been known for some time that photoelectron diffraction is sensitive to local atomic order.<sup>25</sup> By utilizing circularly polarized x rays to generate a localized source of spin-polarized electrons, it is possible to determine local magnetic structure as well. An example of this is shown in Fig. 3, where Fe 2*p* emission has been used to ascertain the local morphology of 4 ML Fe/Cu(001).<sup>26</sup>

Again it is useful to digress to a consideration of the theoretical framework. The theoretical calculation of spin-polarized, multiple-scattering photoemission combines conventional photoemission and spin-polarized low-energy electron-diffraction methods. For calculation of the excitation matrix element,  $\langle \Phi_E | H' | \Phi_E \rangle$ , the nonrelativistic approximation is incorporated and the dipole approximation for the interaction Hamiltonian is used. For this study, the Dirac matrix  $\alpha$  is replaced by Pauli matrices. The selection rules for excitation by circularly polarized light restrict excitations to  $\Delta m_j = +1$  for right-circular polarization and  $\Delta m_j = -1$  for left-circular polarization. The Fe 2*p* core level is split into two sublevels due to the spin-orbit interaction, and transitions from the sublevels are governed by these selection rules. After excitation, the internally polarized photoelec-

trons are multiply scattered inside the crystal in a way similar to spin-polarized LEED electrons. The single-site scattering matrix  $t_{KK'}^{\mu\mu'}$  is calculated using the Dirac equation with spin-polarized potentials generated by a self-consistent linear augmented plane-wave band calculation. This scattering matrix is converted to the (lms) representation and used to construct layer diffraction matrices  $M_{gg'}^{ss'}$ . After that, the calculation proceeds as in a conventional photoemission calculation except that the dimension of the layer diffraction matrices is doubled to include spin-dependent scattering and spin-flip effects. Note that both spin-orbit coupling and exchange effects are accounted for since off-diagonal matrix elements are nonvanishing. In the calculation, the inner potential is set to 10 eV, and inelastic scattering is simulated by an imaginary potential of 4.5 eV. Since the electron kinetic energy is relatively low, only terms up to  $l=4$  are used for most calculations, but convergence is checked using terms up to  $l=6$  with insignificant differences found.

In some respects, this spin-polarized photoelectron diffraction (SPPD) investigation is an independent verification and extension of the pioneering studies of Schütz *et al.*,<sup>27</sup> who used spin-polarized extended x-ray-absorption fine structure (EXAFS) to probe bulk magnetic systems. Consistent with nonspin PD and EXAFS studies, the SPPD shows a larger effect: the SPPD oscillations are on the order of 2%, while the Gd metal SPEXAFS oscillations are  $\leq 1/3\%$ . Additionally, SPPD has the advantage of both energy and angular variations, which is essential to the extension to photoelectron diffraction imaging.<sup>28</sup> Both this work and the ground-breaking studies of Schütz *et al.*<sup>27</sup> are predicated upon control of spin polarization of ejected electrons via excitation with circularly polarized x rays. In a simplistic picture, 2*p* photoemission total cross sections from ferromagnetic materials will exhibit a polarized distribution of 62.5% (37.5%) minority-spin electrons from the 2*p*<sub>3/2</sub> and 25% (75%) minority-spin electrons from the 2*p*<sub>1/2</sub>, when excited with right (left) circularly polarized radiation that is collinear with the magnetic axis of the sample. These adjustably spin-polarized electrons can then scatter off of nearby neighbors, producing a sensitivity to both local geometric and magnetic ordering. (Although we have chosen to use a ferromagnetic system as a test case, these same selection rules will apply in general, e.g., to paramagnetic and antiferromagnetic ordering, and the multiple-scattering analysis should be sensitive to differences in the local order of each structure.) To avoid extraneous effects and to allow internal cross checking of data, measurements were performed only in mirror planes, where only the relative alignment of the photon helicity and magnetization is crucial. Thus reversing the absolute value of these quantities, while maintaining the same relative spin orientation, serves as a convenient but absolutely essential consistency test to determine if the observed asymmetry is due to spin-dependent diffraction. It is the absence of such polarization control or electron-spin detection, plus the ill-defined nature of the intrinsic 3*s* polarization, that has hampered previous attempts at SPPD using the 3*s* level of 3*d* transition metals.<sup>29-31</sup>

## VI. SUMMARY AND CONCLUSIONS

The inherent elemental selectivity and spin sensitivity of MXCD absorption, MXCD photoelectron spectroscopy, and MXCD-photoelectron diffraction make these techniques ideal candidates to study and solve the important interfacial issues in nanoscale magnetism. The future looks particularly bright because of the advent of third generation synchrotron-radiation sources such as the advanced light source. The application of these techniques should provide the detailed information necessary to establish the underlying physics in nanoscale magnetic systems.

## ACKNOWLEDGMENTS

This work was performed under the auspices of the U.S. Department of Energy by the Lawrence Livermore National Laboratory under Contract No. W-7405-ENG-48. The work at Wisconsin was supported by the U.S. Department of Energy under Contract No. DOE DE-FG02-84ER45076. The authors wish to thank Karen Clark for her clerical support. Discussions with James Brug were enlightening and enjoyable. One of the authors (D.P.P.) was supported by IBM Almaden Research during the collaboration.

<sup>1</sup>M. H. Kryder, *Thin Solid Films* **216**, 174 (1992).

<sup>2</sup>J. Brug, Hewlett-Packard (private communication).

<sup>3</sup>B. A. Gurney, V. S. Speriosu, J. P. Nozieres, H. F. Lefakis, D. R. Wilhoit, and D. U. Need, *Phys. Rev. Lett.* **71**, 4023 (1993); B. Dieny, V. S. Speriosu, S. Metin, S. S. P. Parkin, B. A. Gurney, P. Baumgart, and D. R. Wilhoit, *J. Appl. Phys.* **69**, 4774 (1991); B. Dieny, V. S. Speriosu, S. S. P. Parkin, B. A. Gurney, D. R. Wilhoit, and D. Mauri, *Phys. Rev. B* **43**, 1297 (1991).

<sup>4</sup>S. S. P. Parkin, *Phys. Rev. Lett.* **71**, 1641 (1993).

<sup>5</sup>A. C. Ehrlich, *Phys. Rev. Lett.* **71**, 2300 (1993).

<sup>6</sup>V. Grolier, D. Renard, B. Bartenlian, P. Beauvillain, C. Chappert, C. Dupas, J. Ferre, M. Galtier, E. Kolb, J. P. Renard, and P. Veillet, *Phys. Rev. Lett.* **71**, 3023 (1993).

<sup>7</sup>R. Pool, *Science* **261**, 984 (1993).

<sup>8</sup>T. L. Hylton, K. R. Coffey, M. A. Parker, and J. K. Howard, *Science* **261**, 1021 (1993).

<sup>9</sup>*Magnetic Ultrathin Films: Multilayers, Surfaces, Interfaces, and Characterization*, edited by B. T. Jonkers *et al.*, Mater. Res. Soc. Symp. Proc. Vol. 313 (Materials Research Society, Pittsburgh, 1993).

<sup>10</sup>D. Barlett, F. Tsui, D. Glick, L. Lauhon, T. Mandrekar, C. Uher, and Roy Clarke, *Phys. Rev. B* **49**, 1521 (1994).

<sup>11</sup>E. E. Fullerton, M. J. Conover, J. E. Mattson, C. H. Sowers, and S. D. Bader, *Appl. Phys. Lett.* **63**, 1699 (1993).

<sup>12</sup>L. J. Terminello, G. D. Waddill, and J. G. Tobin, *Nucl. Instrum. Methods A* **319**, 271 (1992); J. G. Tobin, G. D. Waddill, Hua Li, and S. Y. Tong, *Mater. Res. Soc. Symp. Proc.* **295**, 213 (1993).

<sup>13</sup>C. Westphal, J. Bansmann, M. Getzlaff, and G. Schonhense, *Phys. Rev. Lett.* **63**, 151 (1989).

<sup>14</sup>J. G. Tobin, G. D. Waddill, and D. P. Pappas, *Phys. Rev. Lett.* **68**, 3642 (1992).

<sup>15</sup>F. U. Hillebrecht, R. Jungblut, and E. Kisker, *Phys. Rev. Lett.* **65**, 2450 (1990); C. L. Roth, F. U. Hillebrecht, H. B. Rose, and E. Kisker, *Phys. Rev. Lett.* **70**, 3479 (1993).

<sup>16</sup>Y. Wu, J. Stohr, B. D. Hermsmeier, M. G. Samant, and D. Weller, *Phys. Rev. Lett.* **69**, 2307 (1992); J. Stohr, Y. Wu, B. D. Hermsmeier, M. G. Samant, G. R. Harp, S. Koranda, D. Durham, and B. P. Tonner, *Science* **259**, 658 (1993).

<sup>17</sup>L. H. Tjeng *et al.*, *Proc. SPIE* **1548**, 160 (1991).

<sup>18</sup>P. Carra, B. T. Thole, M. Alterelli, and X. Wang, *Phys. Rev. Lett.* **70**, 694 (1993).

<sup>19</sup>B. T. Thole, P. Carra, F. Sette, and G. Vanderlaan, *Phys. Rev. Lett.* **68**, 1943 (1992).

<sup>20</sup>N. V. Smith, C. T. Chen, F. Sette, and L. F. Mattheiss, *Phys. Rev. B* **46**, 1023 (1992).

<sup>21</sup>L. Baumgarten, C. M. Schneider, M. Petersen, F. Schafers, and J. Kirschner, *Phys. Rev. Lett.* **65**, 492 (1990).

<sup>22</sup>G. D. Waddill, J. G. Tobin, and D. P. Pappas, *Phys. Rev. B* **46**, 552 (1992).

<sup>23</sup>D. Venus, L. Baumgarten, C. M. Schneider, C. Boeglin, and J. Kirschner, *J. Phys.* **5**, 1239 (1993).

<sup>24</sup>E. Tamura, G. D. Waddill, J. G. Tobin, and P. A. Sterne, *Phys. Rev. Lett.* **73**, 1533 (1994).

<sup>25</sup>S. D. Kevan *et al.*, *Phys. Rev. Lett.* **41**, 1565 (1978).

<sup>26</sup>G. D. Waddill, J. G. Tobin, X. Guo, and S. Y. Tong, *Phys. Rev. B* **50**, 6774 (1994).

<sup>27</sup>G. Schütz *et al.*, *Phys. Rev. Lett.* **62**, 2660 (1989).

<sup>28</sup>J. G. Tobin, G. D. Waddill, Hua Li, and S. Y. Tong, *Phys. Rev. Lett.* **70**, 4150 (1993).

<sup>29</sup>B. Sinkovic and C. S. Fadley, *Phys. Rev. B* **31**, 4665 (1985); B. Sinkovic *et al.*, *Phys. Rev. Lett.* **55**, 1227 (1985); B. Hermsmeier *et al.*, *ibid.* **62**, 478 (1989); E. Zhang *et al.*, *Bull. APS* **39**, 904 (1994). Moreover, there seems to be some revision of interpretation; see Zhang *et al.*

<sup>30</sup>M. T. Johnson *et al.*, *J. Phys. C* **20**, 4385 (1987).

<sup>31</sup>J. G. Tobin *et al.*, in *Advances in Surface and Thin Film Diffraction*, edited by T. C. Huang *et al.*, Mater. Res. Soc. Symp. Proc. Vol. 208 (Materials Research Society, Pittsburgh, 1991), p. 283.